Journal of Cleaner Production 421 (2023) 138467

Contents lists available at ScienceDirect

Journal of Cleaner Production

journal homepage: www.elsevier.com/locate/jclepro

Data driven approach for the management of wind and solar energy integrated electrical distribution network with high penetration of electric vehicles

Manuel S. Mathew [a,*], Mohan Lal Kolhe [a], Surya Teja Kandukuri [b], Christian W. Omlin [a]

[a] University of Agder, Jon Lilletuns Vei 9, 4879 Grimstad, Norway
[b] Norwegian Research Centre, Energy & Technology Department, Tullins Gate 2, 0166 Oslo, Norway

ARTICLE INFO

Handling Editor: Cecilia Maria Villas Bôas de Almeida

Keywords:
Electric grids
Distribution network
Renewable energy fraction
Power prediction
Electric vehicles
Charge discharge scheduling

ABSTRACT

With the increased penetration of fluctuating renewables and growing population of contemporary loads such as electric vehicles, the uncertainties in the generation and demand in the electric power grids are increasing. This makes the efficient operation and management of these systems challenging. Objective of this study is to propose a real-time management system for EV charging, which maximises the renewable energy utilization. An electric power distribution network with an average and peak demands of 1.51 MW, and 3.6 MW respectively, was chosen for the study. The real time power flow through the network components were analyzed using the OpenDSS model. With a wind power density of 574.51 W/m^2 and a solar insolation of 4.14 kWh/m^2/day, an optimized renewable energy system consisting of a 2.3 MW wind turbine and 2.61 MW$_p$ photovoltaic power plant are proposed for the network. Models based on k-Nearest Neighbors algorithms were developed for predicting the performances of these renewable energy systems at the network area. Based on the load profile, power flow analysis, and the predicted generation from solar and wind systems, a demand side management algorithm has been developed for the charge/discharge scheduling of the electric vehicles connected within the network. The basic objective of the algorithm is to maximize the renewable energy utilization by triggering the charging cycle during the periods of excess renewable energy generation. With an annual contribution of renewables is estimated as 12.61 GWh out of which 9.33 GWh is from wind and 3.29 GWh from solar. Wind from wind and solar energy systems, the proposed scheduling algorithm could contribute 71.56 percent of the charging load demand by the EVs.

1. Introduction

For achieving the sustainable development goals of “ensuring access to affordable, reliable, sustainable and modern energy for all by 2030” (Sachs et al., 2022), the global energy scenario has to be shifted more towards carbon free resources and cleaner technologies. As a result, the presence of renewable energy in energy mixes is being significantly increased globally. For example, the global use of renewable energy in electricity generation has reached up to 28% in 2021 (International Energy Agency, 2022b). For tracking the “Net Zero Scenario by 2050”, penetration of renewables in the power grid has to increase by 13% annually till 2030, resulting in a cumulative penetration of 60% of the total generation (International Energy Agency, 2022c). Hence, renewable energy resources and technologies are expected to play a significant role in the global clean energy scenarios.

One of the major challenges in the large-scale integration of renewables sources with electric grids is the intermittence in generation. Resources such as wind and solar are stochastic in nature and could significantly vary with time. In tune with these variations, the power available from these renewable resources would also vary significantly. These uncertainties in the generation could be challenging in the management of the grids, which are already working under the stress from the variabilities in the demand side as highlighted in Impram et al. (2020). One of the solutions proposed to manage these power fluctuations is to use utility scale battery backup (Muqbel et al., 2022; Rouholamini et al., 2022). These systems can support high level penetration

* Corresponding author.
E-mail addresses: manuel.s.mathew@uia.no (M.S. Mathew), mohan.l.kolhe@uia.no (M.L. Kolhe), suka@norceresearch.no (S.T. Kandukuri), christian.omlin@uia.no (C.W. Omlin).

https://doi.org/10.1016/j.jclepro.2023.138467
Received 1 March 2023; Received in revised form 30 July 2023; Accepted 14 August 2023
Available online 18 August 2023

of the variable renewable energy sources into the power grid by storing the excess renewable generation and discharging it during the lean periods. However, large scale and exclusive deployment of storage solutions will add complexities and costs into the system.

Along with the growth in renewable energy use, to further decarbonize the transport sector, electric vehicles (EV) are getting popular in many parts of the world. For example, around 10% of the cars sold globally in 2021 were electric, which is four times the market share in 2019 (International Energy Agency, 2022a). Countries such as Norway has successfully implemented strategies for enhancing the EV population on the roads (Ministry of Transport, 2021). This increasing population of electrically charged vehicles demands matching capacity addition in power generation. One possible way to meet this additional generation capacity sustainably is to integrate more renewable energy systems into the power grids.

Increased presence of electric vehicles in the grids which have high penetration of fluctuating renewables can pose both challenges as well as opportunities. For example, if the charging of these EVs is not properly planned and “controlled”, the additional load brought into the grid by EVs - at the wrong time - could worsen the power quality issues (Taljegard et al., 2019). On the other hand, if the charging is well regulated and matched with the peak renewable energy production, the EVs can be a boon as it reduces the grid pressure and avoids possible RE curtailments. EVs can also function as distributed storage solutions, which get charged and store the excess renewable energy at the peak production periods and discharge it back to the grid during the lean periods. Careful planning, designing, and scheduling are required for successfully implementing such renewable energy prioritized grid systems with substantial EV penetration. With the implementation of such ‘smart’ solutions, EVs and grid systems can be made mutually supportive.

A comprehensive review on various methods for optimal EC charging scheduling, based on more than hundred studies, is presented in Ali Saadon et al. (2019). Potential benefits and risks of various strategies in scheduling the charging of electric vehicles are identified in this review. The study indicates that most of the research in EV charge scheduling focuses on the centralized control approach, where an aggregator controls and decides the charging schedule of the EVs (Alsabbagh et al., 2020, 2021; Kapoor et al., 2022). The computational and communicational infrastructure, and the resulting costs are high in such centralized charging approaches (Zhao and Ding, 2017). With the fast increase in EV population, scalability and management of data could also be challenging for the centralized approach (Rahbari-Asr and Chow, 2014). Further, centralized charging can limit the satisfaction fairness among the EV users in terms of SOC (Aswantara et al., 2013) and could pose privacy challenges due to the sharing of several private information which are required for the centralized control (Zhao and Ding, 2017). A solution for resolving the above issues is a decentralized and cooperative charging approach (Paudel et al., 2022). The present study proposes such a decentralized charge scheduling in which the charge-discharge scheduling is controlled at the user community level.

In most of the previous studies, EV charge scheduling algorithms are optimized with the objectives of either smoothening the grid load (Moeini-Aghtaie et al., 2014; Van Kriekinge et al., 2021), or minimizing the cost (Triviño-Cabrera et al., 2019; Visakh and Selvan, 2021; Zhao and Ding, 2017). A few studies with the main objective of maximizing the renewable energy fraction in EV charging have been reported recently. Out of these, most studies propose storage solutions like batteries to maximize the renewable energy fraction as seen in Alghoul et al. (2018), Himabindu et al. (2021), Allouhi and Rehman (2023), and Bilal et al. (2023). Reasonably high renewable energy fractions are reported under these studies. In some other analysis, supplementary generation systems like diesel generators are used to handle the fluctuations in renewable energy generation (Boddapati et al., 2022; Singh and Kumar, 2023). Possibilities of using biogas generators is also explored for increasing the renewable energy share (Ampah et al., 2022). In view of the obvious technical and economic challenges in using large scale battery backup in EV charging, a few recent investigations propose charging systems without any storage or generation backup options (Rehman et al., 2023; Ullah et al., 2023; Zhang et al., 2023). However, the renewable fraction reported under these studies are significantly lower compared to the approaches with storage and other supplementary generation options.

Novelty and contribution of the study is discussed below:

1. The major objective of this study is to maximize the renewable energy fraction in charging the EVs connected to renewable integrated power distribution networks. In contrast with the previous studies reviewed above, this is achieved without the support of any battery storage or backup generation systems as seen in Table 3. For maximizing the renewable energy fraction, the proposed smart EV charging algorithm schedules the charging of EVs prioritized during the periods of higher renewable energy generation, depending upon the state of charge (SOC) of the EVs.
2. Real time power flow in the distribution network is modelled and considered in the EV charge scheduling, which, as far as the authors knowledge, is not included in the previous studies.
3. While in the previous studies, physical models are used for estimating the generation from the renewable energy systems, in this study renewable energy production is estimated using machine learning based algorithms. This helps in using realistic estimates of renewable contributions in the analysis (Veena et al., 2020).
4. In the proposed decentralized and community-based EV charge scheduling, a wholistic approach is adopted, which consider all the influencing parameters such as the load flow in the network, renewable energy availability & sizing and the state of charge (SOC) the EVs.
5. The algorithm we propose can adapt to different practical situations by modifying parameters such as the number and locations of the EVs, the battery capacity, connection status, state of charge, discharging agreements and so on.

After this introductory section, features of a candidate power distribution network with which the proposed system can be demonstrated are presented. Wind and solar energy resources, which can possibly be integrated with this network are then quantified and corresponding generation systems are sized. Intelligent models, which can predict the power generation from these renewable energy systems are then presented. Finally, a demand side management algorithm for the smart charge/discharge scheduling of the EVs connected to the network is presented.

2. The power distribution network and load analysis

2.1. The distribution network

A test distribution network near to Iowa State University has been chosen (Bu et al., 2019) for demonstrating the proposed smart energy management system. Three reasons motivated our choice of this network: (i) the system architecture and the load data of this network, which are required for the study were made available. (ii) The network was found to be an ideal candidate for modernization through renewable integration, and (iii) there are possibilities of high EV penetration in the region. The test network is a radial distribution network and consists of 3 feeders and 240 nodes which are supplied by a 69-kV substation. Schematic of the test system is shown in Fig. 1. There are 1120 customers connected to this network and the connections are equipped with smart meters. The energy demands of customers are aggregated at the respective secondary transformer level. Based on the time series distribution data, the real and reactive load profiles at each node were computed.

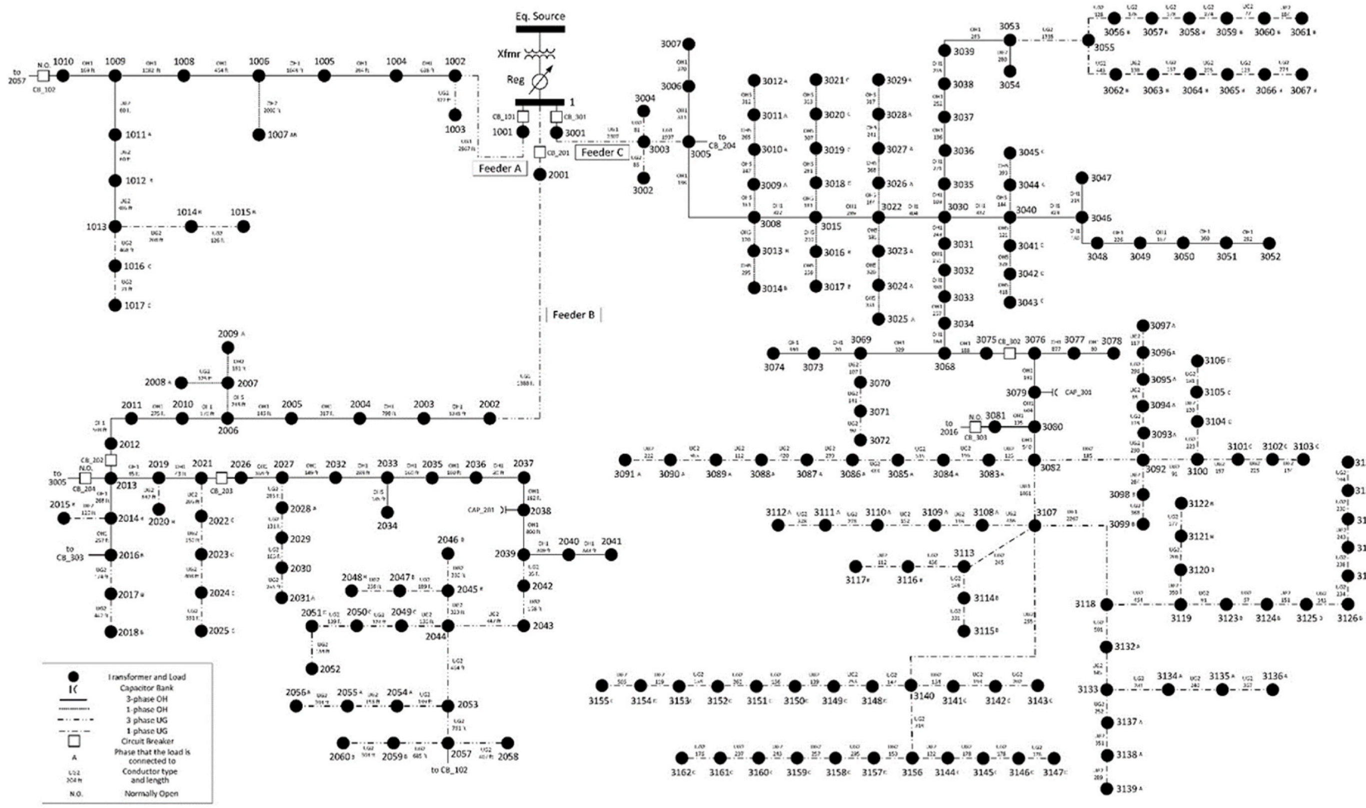

Fig. 1. The 240-Bus distribution test network used for the study (Bu et al., 2019).

2.2. Analysis of the load

The hourly variations in the load experienced in the network in different months are shown in Fig. 2. The shaded region represents the region of ±25% variations from the average load. As expected, significant variations in the hourly load were observed during all the months. The highest recorded load over the year was 3595.5 kW and the lowest load was only about 19% of the peak. Based on this, the average load profile of the network during different hours of the day were computed and presented in Fig. 3. As expected, the load is relatively high between 08:00 to 20:00 with peaks between 10:00 and 12:00. On average, the peak load on the system is 1871.4 kW whereas the lowest was 969.47 kW. This general pattern differs slightly during the months, depending on the seasonal and other weather variations.

Further, the power flow through different components of the distribution network was simulated using the Open Distribution System

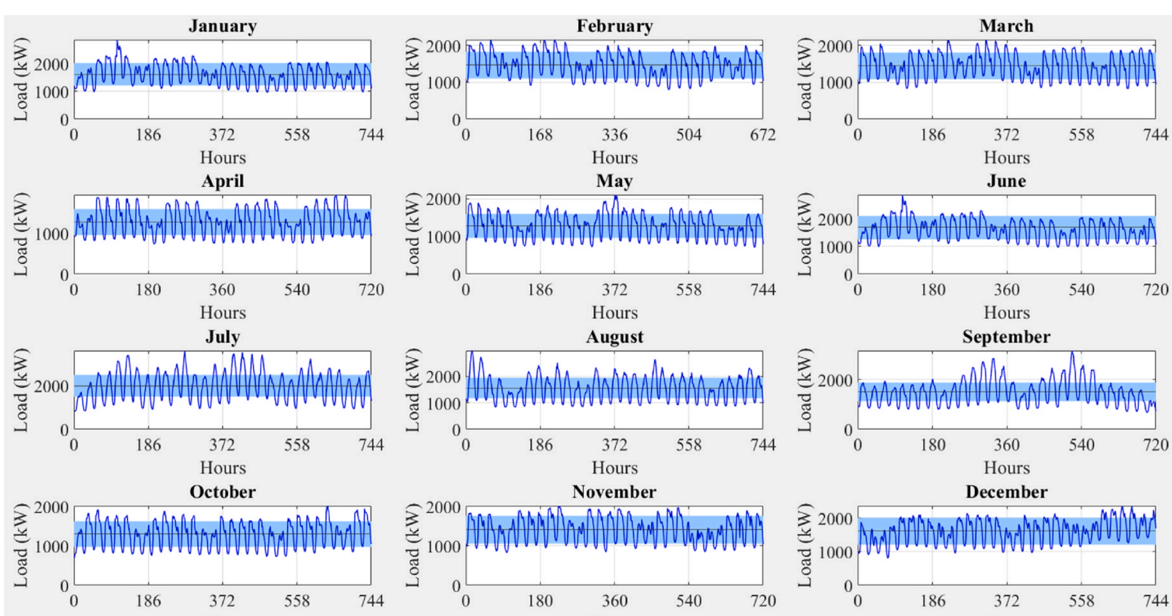

Fig. 2. Hourly load variations during the months.

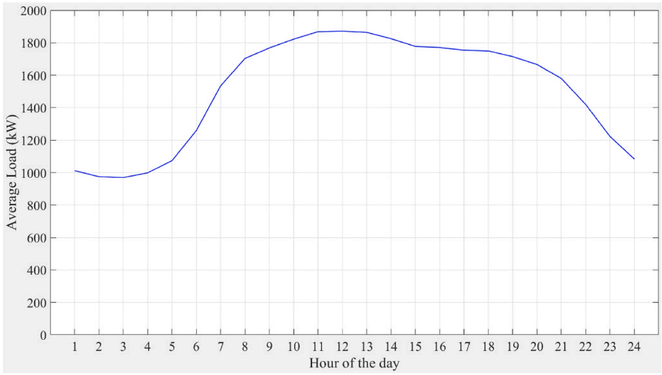

Fig. 3. Hourly load variation in a day.

Simulator (OpenDSS) (Ramachandran, 2011). The provision in OpenDSS to design and execute power flow simulations through third party programs using its COM interface was utilized for this study. Accordingly, the simulations were activated and called through custom made codes. The output results of this model implementation are the line current, bus voltage (both in magnitude per unit and in rectangular coordinates), line power (both active and reactive) and losses in various elements. The model was implemented at each step of the EV charge simulations and the results were used in the smart scheduling of the EVs with renewable energy prioritization.

3. Renewable energy resource estimation and sizing

3.1. Renewable energy resources

One of the major focuses of the current research is to transform the studied network to a 'greener and sustainable' system through significant integration of renewable energy generators with the network. Quantifying the renewable energy resources available at the region available at the region is essential for efficient integrations. Based on the meteorological data, wind and solar energy were identified to be suitable for the region. These resources at the site are quantified as discussed below.

3.1.1. Wind energy

Hourly wind data for the location was collected over seven years (Iowa State University, 2021), which are then extrapolated to that corresponding to the hub height of a prospective wind turbine using the logarithmic law (Mathew, 2006). Annual average wind speed at the site was 7.7 m/s, with a standard deviation of 4.58 m/s. Though the wind speed shows significant variations, in general, the site has reasonably good wind potential. The distribution of wind at the site is characterized by the Weibull distribution with its Probability density ($f(V)$) and cumulative distribution ($F(V)$) given by:

$$f(V) = \frac{k}{c}\left(\frac{V}{c}\right)^{(k-1)} e^{-\left(V/_c\right)^k} \tag{1}$$

and

$$F(V) = \int_0^\alpha f(V)dV = 1 - e^{-\left(V/_c\right)^k} \tag{2}$$

where k is the Weibull shape factor and c is the Weibull scale factor. From the average and standard deviations of wind velocities, k and c for the site were calculated using (Mathew, 2006):

$$k = \left(\frac{\sigma_V}{V_m}\right)^{-1.090} \tag{3}$$

and

$$c = \frac{2V_m}{\sqrt{\pi}} \tag{4}$$

Weibull shape factor k and scale facto c, computed for the region were 1.47 and 8.32 m/s respectively. The relatively lower shape factor indicates high variations in wind speed at the site. Similarly, the reasonably strong wind potential available at the site has been reflected in the scale factor. Probability density and cumulative distributions of wind velocity at the site are shown in Figs. 4 and 5, respectively.

One of the important indicators for wind energy potential is the wind energy density. The annual averaged wind energy density at the site is 574.51 W/m^2. This high wind energy density clearly indicates the viability of wind energy generation at the site.

3.1.2. Solar energy

For quantifying the solar resource available at the site, hourly Global Horizontal Irradiance (GHI) data and the corresponding ambient temperature were collected (Iowa State University, 2021). Based on these data, the solar resources available at the site have been statistically analyzed.

The annual average daily solar insolation at the site was 4.14 kWh/m^2/day. The solar resources at the site were modelled using probability distributions. In contrast with the case of wind, there are no standard distributions which can be universally used to represent the solar resource. Hence the data were fitted with some potential distributions and the goodness of fit were tested with Kolmogorov Smirnov, Anderson Darling, and the chi-squared tests. Beta distribution was found to represent the solar resource available in the region. The probability density and cumulative distribution functions of Beta distribution is given by:

$$f(x) = \frac{B_x(\alpha,\beta)}{B(\alpha,\beta)} \tag{5}$$

and

$$F(x) = \frac{x^{\alpha-1}(1-x)^{\beta-1}}{B(\alpha,\beta)} \tag{6}$$

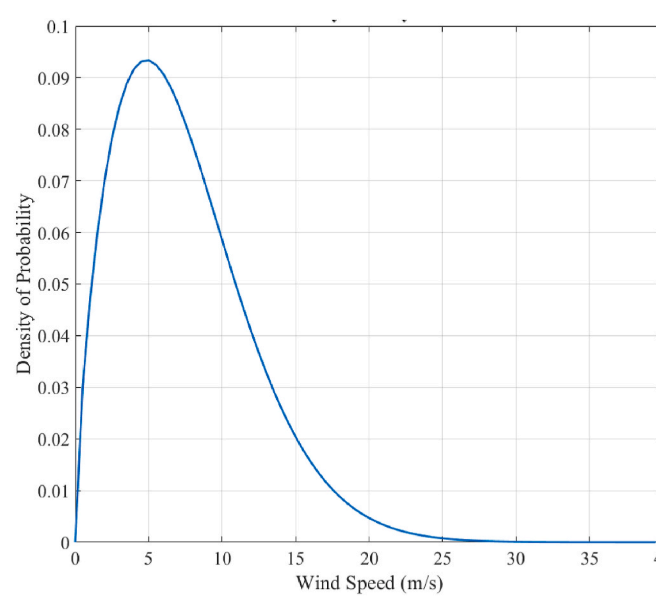

Fig. 4. Probability densities of wind speeds at the site.

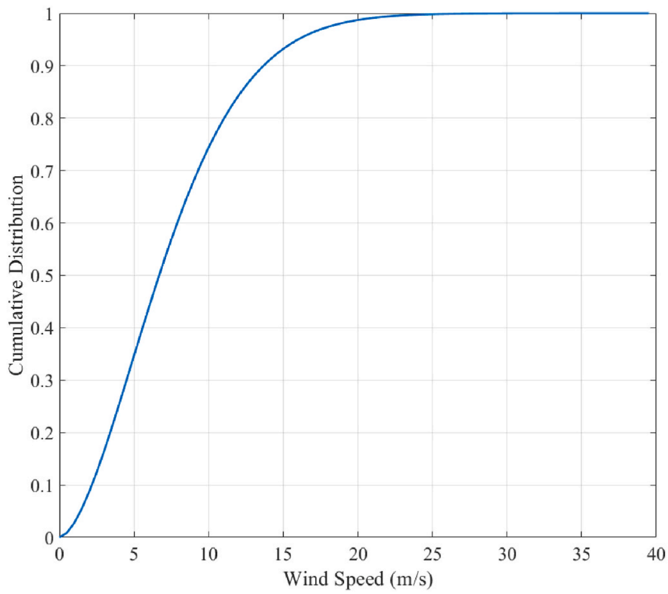

Fig. 5. Cumulative distribution of wind speeds at the site.

where B is the Beta Function, and B_x is the Incomplete Beta Function. Here α_1 is the continuous shape parameter ($\alpha_1 > 0$), α_2 is the continuous scale parameter ($\alpha_2 > 0$) and a, b are continuous boundary parameters ($a < b$) $a \leq x \leq b$. Solving from the data, the continuous shape, scale parameters are 0.73 and 1.40, respectively. The boundary parameters considered are 1 and 1014, respectively. Based on this, the probability density and cumulative distribution of solar irradiance were computed, which are shown in Figs. 6 and 7, respectively.

3.2. Optimal renewable energy system

The above analysis on the wind and solar energy resources available at the site indicates the potential of exploiting these resources for possible energy generation in the region. Based on the same data as discussed above, and considering the load profile presented in Section 2.2, the size of renewable energy systems to be integrated with the network was optimized using the Hybrid Optimization of Multiple Energy Resources (HOMER) Model. Economic, environmental, and the technological aspects of the proposed power system with renewables are considered in the optimization. Under the optimization, various possible configurations of the system are simulated. The system configuration which satisfies all the technical constraints and has the lowest life-cycle cost is chosen through grid search algorithm. The architecture of the proposed system is shown in Fig. 8. Features of the wind and solar system considered are highlighted in Table 1.

Under the optimization, various economic and environmental parameters of the proposed system under different operational constraints are analyzed and the optimal configuration of the hybrid system was identified. The optimized renewable energy system consists of a wind turbine of 2.3 MW capacity and 2.6 MW_p solar PV (Photo-Voltaic) system.

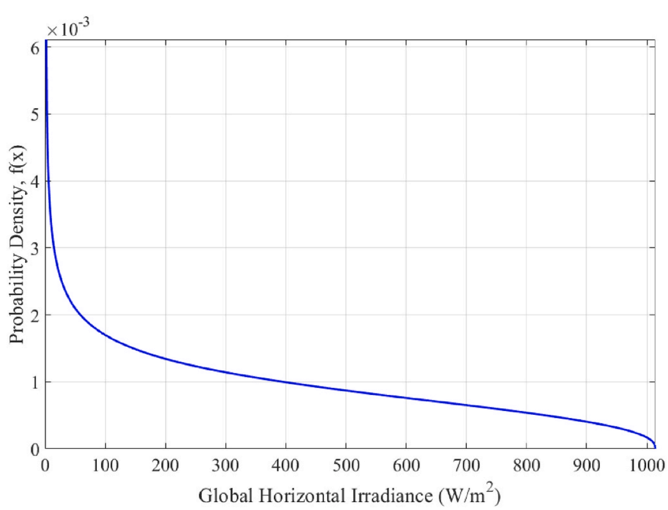

Fig. 6. Probability density function of solar energy resource.

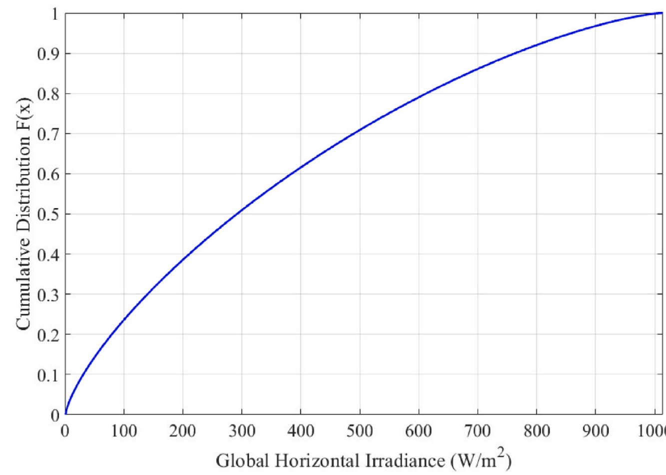

Fig. 7. Cumulative distribution of solar energy resource.

4. Machine learning based performance models for the renewable energy systems

4.1. Data preprocessing and model development

Site specific performance models, based on machine learning (ML), has been developed under the study for predicting the performance of

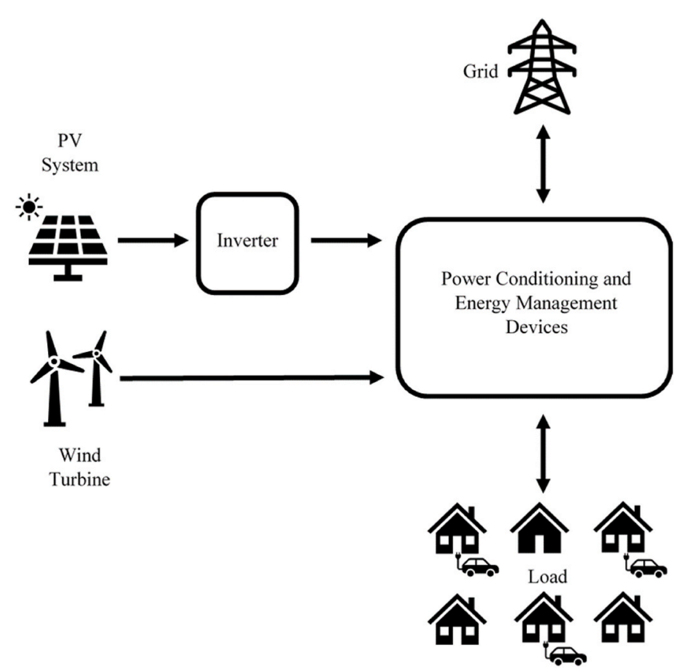

Fig. 8. Architecture of the renewable energy integrated distribution network.

Table 1
Features of the renewable energy systems considered in the optimization.

Wind turbines	2.3 MW rated capacity, lifetime 25 years
Operational wind velocities of the turbine	Cut-in 3.5 m/s, rated 15 m/s, cut-out 25 m/s.
Performance model for the turbine	Manufacturers power curve
PV system	Monocrystalline panels,
PV system efficiency	19.4%
Invertor and rectifier efficiencies	95%

the proposed wind and solar energy systems in different time intervals. These models could estimate the share of renewable energy in the energy mix at a given time and thus can be used for developing the smart Charge/Discharge Scheduling algorithm for the EVs.

To develop the performance model, operational data from a 2.3 MW wind turbine and a PV power plant, working under similar environments of the candidate site, were collected (It should be noted that this data was used only to develop the ML models for wind and solar systems. Once these models are developed, performance of these systems at the proposed network region is simulated using the weather parameters collected from the site as discussed under Section 3.1). The data collected were initially cleaned for eliminating errors and missing data points. Further, the outliers of the data were identified and removed using Z-score and DBSCAN based anomaly detection methods (Ester et al., 1996). The former was used for removing the extreme outliers in contrast with the latter. The combination successfully detected and removed the outliers.

After cleaning the data, the features of the dataset significant for the ML based performance models for wind turbine and PV module were identified. The data for wind turbine modelling included the features viz. the wind velocity and wind direction as well as the output power generated by the turbine. The data for PV module modelling included the features like the solar irradiation at 45°, GHI, wind velocity, precipitation, ambient temperature, and the output power generated by the module. For evaluating the significance of these features on the performance models, the data were analyzed with Pearson and Spearman correlations. The prediction models for the wind and solar energy systems were developed with these identified features. Though several ML algorithms were initially considered, the k-Nearest Neighbors regression (kNN) (Fix and Hodges, 1989) performed best in predicting the performance of both the wind turbine and the PV system and hence was chosen for further analysis.

The model that best describes the wind turbine or the PV systems depends on the value of *k*. Thus, an optimum value of *k* is to be selected. For this, a grid search algorithm with 10-fold cross validation was used. The grid search algorithm iterates over the value of k from 1 to 100 searching for the value of *k* that results in the lowest error values. Using the selected value of *k,* we train the performance models of wind turbine and PV module using 10-fold cross validation on the training dataset.

Finally, the model thus trained has also been tested on an entirely different set of data that has not been presented to the model in the training phase. Accuracies of these models are assessed with error metrics like Root Mean Square Error (RMSE), Normalized N Root Mean Square Error (NRMSE) and the coefficient of determination (R^2), where:

$$RMSE = \sqrt{\frac{1}{N}\sum_{i=1}^{N}\left(\hat{y}_i - y_i\right)^2} \tag{7}$$

$$NRMSE = \frac{RMSE}{\left(y_{(\max)} - y_{(\min)}\right)} \tag{8}$$

$$MAE = \frac{1}{N}\sum_{i=1}^{N}\left|\hat{y}_i - y_i\right| \tag{9}$$

$$R^2 = 1 - \frac{\sum\left(y_i - \hat{y}_i\right)^2}{\sum\left(y_i - \bar{y}_i\right)^2} \tag{10}$$

where N is the total number of datapoints, y_i is the observed power, $\hat{y}_i$ is the predicted power and $\bar{y}_i$ is the mean value of actual power, whereas $y_{(\max)}$ and $y_{(\min)}$ is the maximum and minimum value of observed power.

4.2. Wind turbine model

Under the Pearson and Spearman correlation tests, correlation between the wind speed and power produced by the turbines were found 0.94 and 0.99 respectively. All other considered parameters, including the wind direction showed negligible correlation with the power. Hence, the wind speed has been chosen as the single feature for the k-NN model. Under the tenfold cross validation method by implementing the grid search algorithm, the optimum value of k for the wind turbine model was estimated as 30. Thus, the model was trained with $k = 30$ and was tested with the test dataset.

Results of the model performances for representative days are shown in Fig. 9. The model could perform well in estimating the power developed by the turbine at different wind velocities. The slight variations between the predictions and observations can be seen at the peaks of these figures. It could be noted that these peaks correspond to sudden changes in the wind, which could affect the accuracy of the wind measurements as well. Model performance, considering the whole test dataset are illustrated in Fig. 10. Close agreements between the predictions and real observations can be seen. The model showed an RMSE of 71.84 kW and NRMSE of 0.03. The corresponding MAE and R^2 were 39.91 kW and 0.99 respectively. These clearly indicate the capability of the proposed kNN based performance model in characterizing the performance of the turbine.

4.3. PV system model

Under the Pearson and Spearman correlation tests, power output of the PV system is found to be significantly correlated with the global horizontal irradiance and ambient temperature. Thus, these are chosen as the input features for the solar PV model. Based on error tests, a *k* value of 27 was chosen for the model which was developed and tested with the test data set. Measured outputs of the solar PV system during a representative day and the corresponding outputs predicted by the model are compared in Fig. 11. Except for the peaks, good agreement can be observed between the measurements and model predictions. This is further reconfirmed in Fig. 12, where the performance of the model is demonstrated with the complete test dataset. RMSE, NRMSE and MAE of

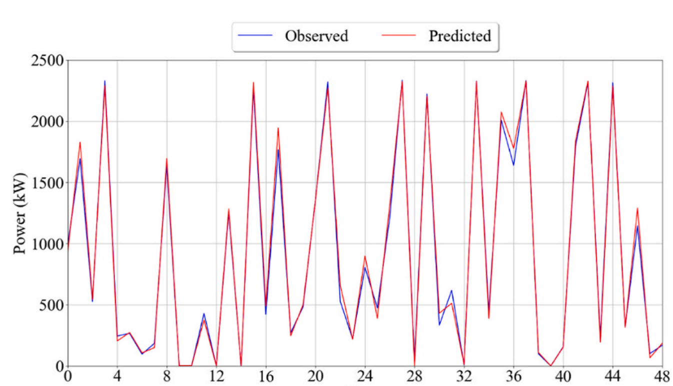

Fig. 9. Comparison of the kNN power prediction with the actual observations from the test dataset.

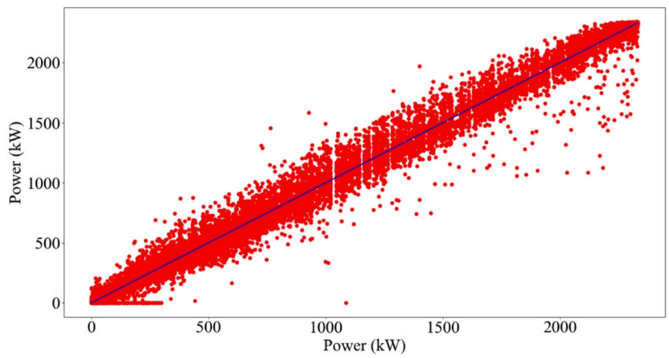

Fig. 10. Comparison of predicted and observed power for wind turbine.

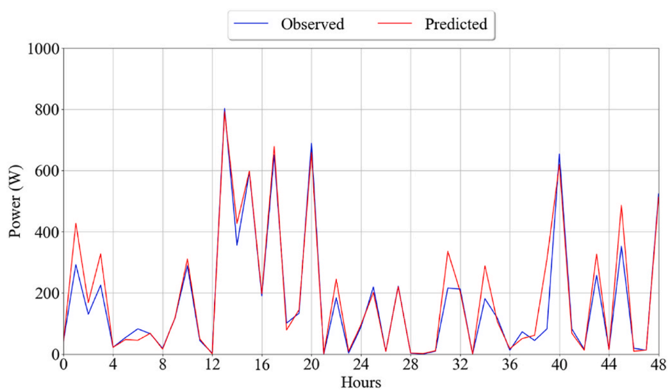

Fig. 11. Comparisons of the power predicted and observed output of the solar PV system.

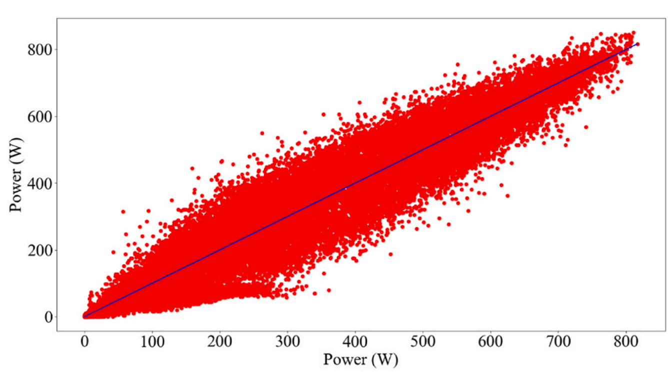

Fig. 12. Comparison of predicted and observed power for the solar PV system.

the k-NN based model under these tests are 54.03 W, 0.06 and 35.23 W, respectively. It may be noted that the model was developed and tested with the performance data of the PV system, normalized to a unit panel size of 1 kW. The corresponding R^2 of the model is 0.94.

5. EV charge scheduling

For charging of the EVs within the proposed network with maxim fraction of renewable energy resources, and to supplement the grid during lean renewable energy generation, a smart EV charging algorithm is proposed under this study. The aggregated load demand is computed in this approach considering the typical variation of the EV loads. Flow chart of the proposed EV Charge/Discharge scheduling algorithm is shown in Fig. 13. The scheduling of the EVs is done on a distribution network level in which the customers who draw power from

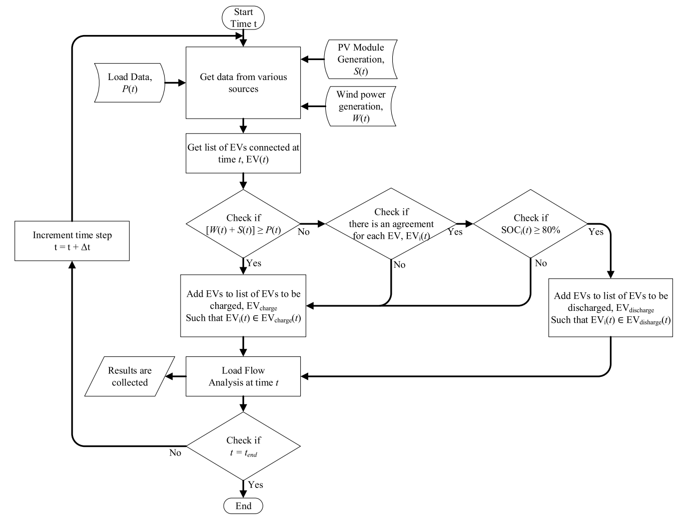

Fig. 13. Flow chart of the EV charge/discharge scheduling algorithm.

a primary distribution transformer come together to form a consortium to make agreements with individual EV owners that states whether their EVs can be used both in grid-to-vehicle mode and vehicle-to-grid mode, depending on the needs of the grid and the charge status of the EVs, or only in Grid-To-Vehicle mode. The working of the scheduling algorithm is described below: The algorithm starts at a time, t. Initially, the data from various sources are collected. From the performance model of the PV Module, we get the generation ($S(t)$) from the PV module at time, t. From the performance model of the wind turbine, we get the generation ($W(t)$) from the wind turbine at time, t. And finally, the load ($P(t)$) at time, t from the Load Data. Now, a list (EV(t)) is generated based on which EVs are connected at time, t. This list includes four parameters for each EVs which indicates (i) if the EVs are connected or not, (ii) if the connected EVs have an agreement to be operated in Vehicle-To-Grid mode with the consortium or not, (iii) the state of charge (SOC) of the EVs, and (iv) node number at which the EV is connected.

It is assumed that there are 80 EVs under the distribution network, which are randomly distributed throughout the 240 nodes. While in practical implementation, this can be changed flexibly, as the exact number of EVs in the distributed network can be included in the algorithm. The EVs connected during a time step, t is assumed to stay connected for the duration of Δt. It is assumed that in scheduling charging/discharging of EVs for a typical day, conditions given in Table 2 is applicable. While practically implementing this code, the number of EVs connected at a given time can easily be detected using appropriate sensing devices.

It is also assumed that EVs disconnected in each time step, Δt has its SOC drop by 5–20% of its initial SOC at random, except between 09:00 and 18:00. This is to account for the randomness in the usage of EVs which is dependent on several factors like kilometres driven, terrain

Table 2
Connection/disconnection pattern of EVs during a workday.

No.	Time	Condition
1	00:00 to 05:00	78 EVs are connected at any given time step while 2 EVs disconnect randomly to account for emergency uses of the EV.
2	06:00 to 08:00	60 EVs are connected at any given time step with 20 EVs disconnected at random.
3	09:00 to 17:00	5 EVs are connected at any given time step and 75 EVs remain disconnected throughout the duration accounting for EVs in use.
4	18:00 to 21:00	40 EVs are connected at any given time step with 40 EVs disconnected at random.
5	22:00 to 00:00	78 EVs are connected at any given time step while 2 EVs disconnect randomly to account for emergency uses of the EV.

driven on, weather, etc. The state of charge (SOC) is defined by:

$$SOC(t+\Delta t) = SOC(t) - x{\cdot}SOC(t) \tag{11}$$

where x is the percentage drop in SOC between 5% and 20% selected at random for each EV. Between 09:00 and 18:00, it is assumed that the SOC of the disconnected EVs drop to 60%–80% at random. All the EVs in the distribution network are assumed to have the same battery capacity of 36 kWh and have a charge/discharge rate of 3.6 kW. For practical implementation of the code under different situations, when the exact battery capacities of the EVs are known, all these assumed parameters can be changed within the code. It is assumed that the EV has a charging efficiency, η_{charge} of 80% (Apostolaki-Iosifidou et al., 2017) and the SOC of EVs have been updated using the equation derived from Sharma (2021) as:

$$SOC(t+\Delta t) = SOC(t) - \frac{\eta_{charge}\left(P_{charge}{\cdot}\Delta t\right)}{E_{Battery}}{\cdot}100 \tag{12}$$

where P_{charge} is the rate at which the EV battery is charged, $E_{Battery}$ is the total energy capacity of the EV battery. The EV is considered to have a discharging efficiency, $\eta_{discharge}$ of 80% (Apostolaki-Iosifidou et al., 2017) and the SOC of EVs have been updated using the equation derived from Sharma (2021) as:

$$SOC(t+\Delta t) = SOC(t) - \frac{P_{discharge}(t){\cdot}\Delta t}{\eta_{discharge}{\cdot}E_{Battery}}{\cdot}100 \tag{13}$$

where $P_{disharge}$ is the rate at which the EV battery is discharged and $E_{Battery}$ is the total energy capacity of the EV battery.

The existing load profile and the power flow within the network, along with the power prediction for the wind and solar PV systems were considered in this scheduling. The load on different system components including the EVs, at each time of interest, has been analyzed by activating the OpenDSS model. Possible losses in different subsystems are accounted in this analysis.

The power demand of a small group of residential units are catered by each node. As discussed, these residents are assumed to own 80 EVs. To mimic the presence of EVs in these units, 0–3 EVs are randomly distributed over different nodes. These numbers and distribution pattern can be changed in the algorithm to match any situation of EV charging.

6. Results and discussion

Results of the major objectives of this work, which is renewable energy prioritization while charging to maximize the renewable energy fraction, are presented and discussed in the following sections.

6.1. Renewable energy prioritization

The proposed ML models, discussed under Section 4 are used to estimate the generations from wind and solar energy systems. Various inputs required for these models are taken from the data collected from the region of the proposed network as discussed in Section 3. Hourly contribution in power from the renewable energy generation for a representative day is shown in Fig. 14. As expected, there are high variations in the renewable energy contribution in different hours. The generation pattern can also change with the weather and seasonal variations.

Generations from the solar and wind energy systems, on a monthly basis are shown in Fig. 15. As we can see, the major contribution in renewable based electricity generation comes from the wind turbine. The total generation from the renewables varies significantly from month to month. The generation is highest in the months of May and June, whereas the summer months are leaner in renewable energy contributions. This is mainly because of weaker wind resources during the summer months. It may be noted that even during the summer months, the solar resource is stronger, which is reflected in the PV system contributions indicated in the figure.

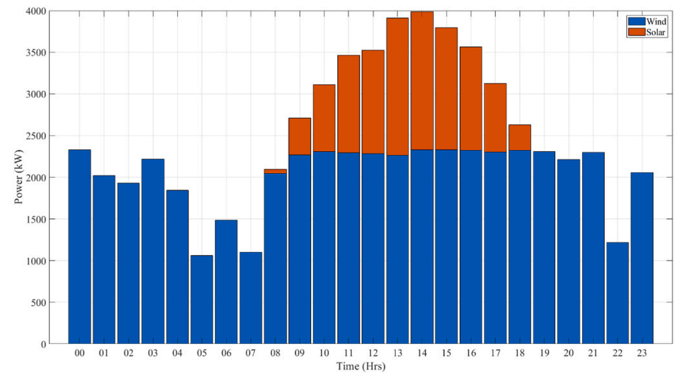

Fig. 14. Hourly generation of renewable energy on a typical day.

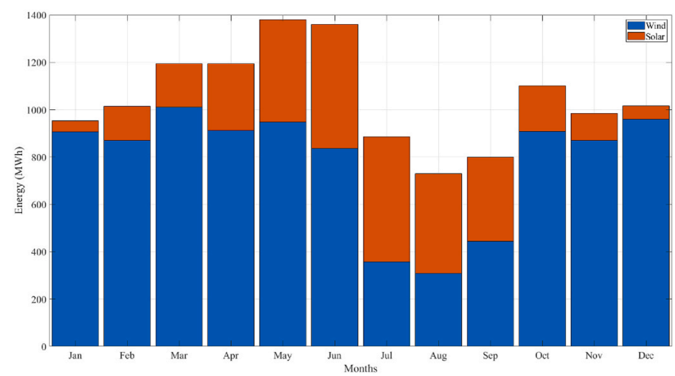

Fig. 15. Monthly generation from the wind and solar energy systems.

For further investigating the renewable energy prioritization of the proposed system, scenarios of generation before and after the renewable energy systems integration are compared in Fig. 16. Scenario 1 represents the system before integrating the wind turbine and solar PVs. In this scenario, the complete demand on the network, in all the months, is met through grid purchases. In contrast, in scenario 2, which represents the system after the renewable energy integration, the grid purchase has significantly reduced. Additionally, in the months of March, April, May, June and October, excess renewable generation could be sold to the grid, which makes the option economically attractive. This again is a clear indication of the grid support and renewable energy prioritization of the proposed system.

On an annual basis, renewables would contribute 12.61 GWh to the

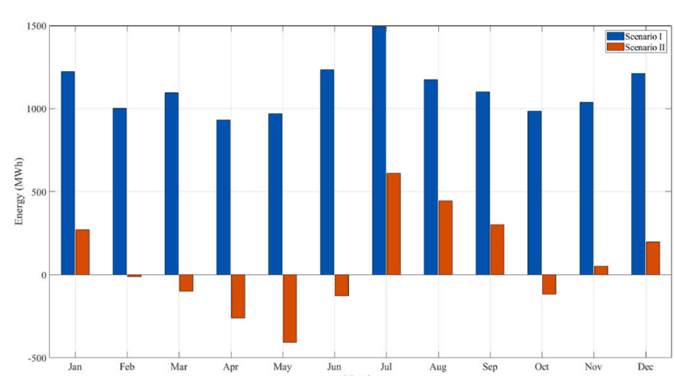

Fig. 16. Comparison between the scenarios before and after renewable energy integration.

proposed system. Out of this, the share of wind would be 9.33 GWh whereas the solar production would be 3.29 GWh.

From these, it is evident that the proposed system would have significant presence of electricity generated from sustainable resources.

6.2. EV charging schedule

Out of the 80 EVs connected to the network, owners of 60 EVs are assumed to have agreement with the management system for discharging power back to the grid while the renewable generation is not sufficient to meet the load at a given time. Though the EVs with discharging agreement is arbitrarily fixed for the simulations, this is flexible and can be changed for any charging scenarios as needed. Among the EVs with charge-discharge agreement, the discharge is permitted only at an SOC of 90% or above.

The typical averaged power taken from the grid by the EVs for charging and given back to the grid while discharging, in different hours during a representative day, is shown in Fig. 17. The total energy consumed in the day for charging is 2335.4 kWh. The EVs could discharge 540 kWh back to the grid during the periods of lean renewable energy contribution. This indicates the functioning of the charge-discharge cycle as expected for the proposed system. However, for keeping a steady SOC of 90%, the EVs are mostly on the charging mode. As a result, the power contributions back to the grid are minimal.

To understand the effect of SOC restrictions on the charge-discharge cycle, the SOC level of the EVs, on the same day, has been varied at 75% and 60%. The resulting charge discharge rate is shown in Figs. 18 and 19, respectively. At 75%, daily charging would be at a level of 2392 kWh. Corresponding daily discharge would be at 727.2 kWh. However, when the SOC restriction is changed to 60%, corresponding this would change to 2181.4 kWh and 964.8 kWh, respectively. This indicates the sensitivity of the charge-discharge cycle on the levels the SOC restrictions. Nevertheless, these restrictions can be flexible and can be varied at different levels as required.

Overall picture of the power flow over the network with renewable prioritized generation options and under the 'smart' EV charging schedule for three different days in a year is displayed in Fig. 20. In the figure, power corresponding to the positive side represents the average hourly load on the network (including that for EV charging) which is contributed by the power purchased from the grid, generated by the wind turbine and the solar PV system, and the power discharged back by all the EVs. The negative values indicate the sales of excessive renewable power back to the grid. From the figures, it is evident that the system is predominantly dependent on renewable resources like wind and solar to meet its power demand and thereby could make the conventional network a cleaner and greener system. In addition, sales of excess renewables back to the grid can make the system economically attractive.

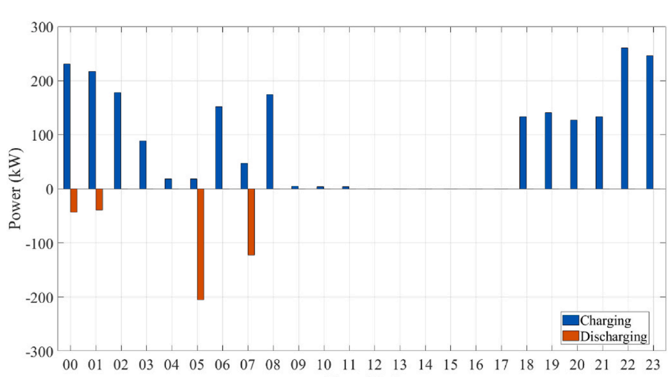

Fig. 17. Hourly charge-discharge rate of EVs with 90% SOC restriction.

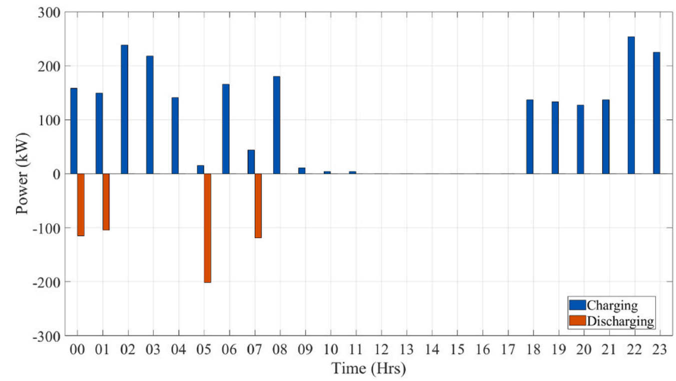

Fig. 18. Hourly charge-discharge rate of EVs with 75% SOC restriction.

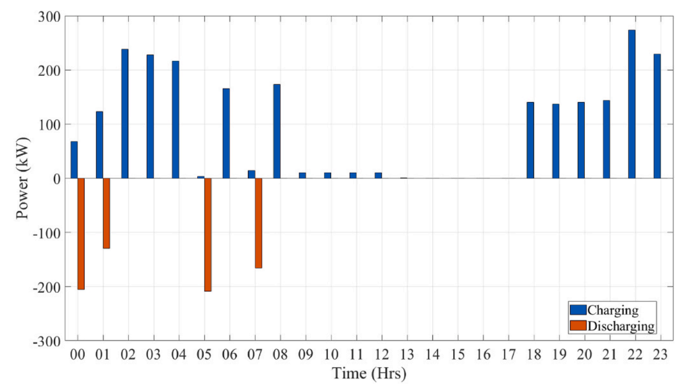

Fig. 19. Hourly charge-discharge rate of EVs with 60% SOC restriction.

6.3. Comparison with similar studies

One of the main objectives of this study is to maximize the share of renewable energy in meeting the EV charging. Hence, it is interesting to compare the performance of the proposed charge scheduling algorithm with similar studies. Though there are several reported research on EV charge scheduling, only a few studies are focused on maximizing renewable energy fraction. Details of some of these recent studies are listed in Table 3. The size of the renewable energy systems and other components are economically optimized in all these investigations. These studies are of two categories (1) studies in which storage batteries or other backup generating options are included for maximizing the renewable energy fraction (2) studies without considering such storage or generation options. As seen from the table, relatively higher renewable energy fraction is reported when battery and supplementary generation options are considered. However, in the present study, such backup solutions are not considered due to obvious techno-economic reasons. It can be seen that, even without the power backup solutions, the proposed charge scheduling approach could enhance the share of renewable energy in EV charging to an impressive 71.56%, which is higher than the fraction reported in similar studies.

7. Conclusions

In this study, we propose a smart EV charge scheduling algorithm, which can maximize the renewable energy fraction in EV charging, without any battery storage or supplementary power options like diesel generators. A distribution network with average and peak demands of 1.51 MW and 3.6 MW respectively was chosen for the analysis and power flow through various components of the distribution network has been analyzed using OpenDSS. With an estimated 574.51 W/m^2 of wind power density and 4.14 kWh/m^2/day of solar insolation at the network

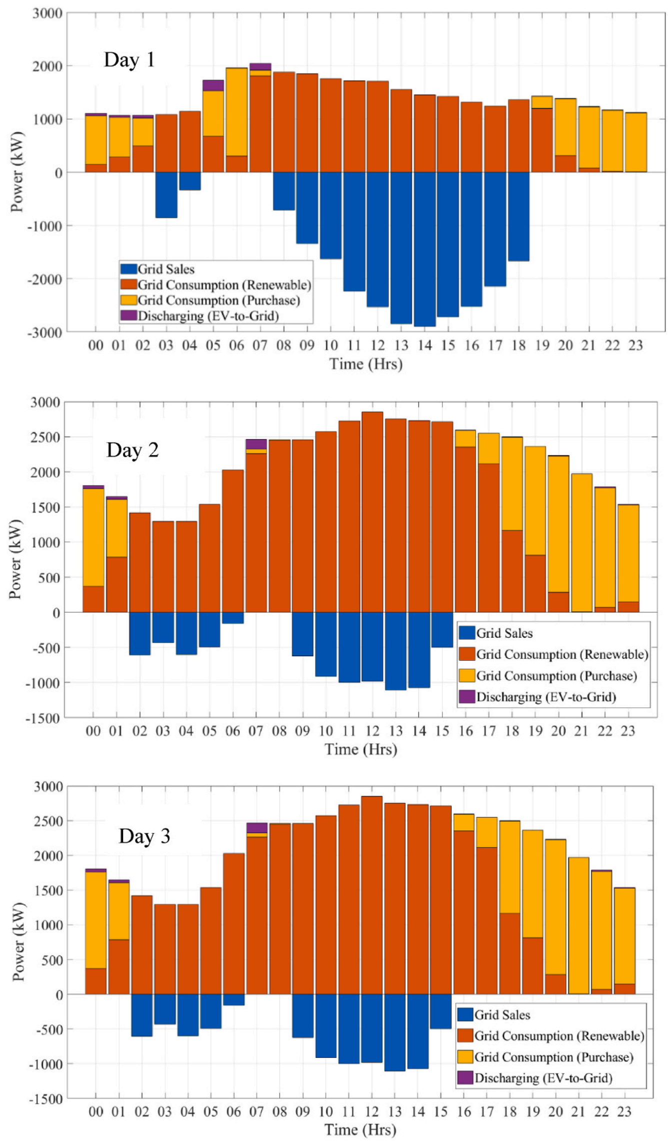

Fig. 20. Overall power flow based on the proposed scheduling scheme on three representative days.

region, an optimum renewable energy system consisting of a 2.3 MW wind turbine and an aggregated 2.6 MW solar power plant is proposed for the network. kNN based machine learning models are developed for estimating the power output of these renewable energy systems which estimates a total contribution of 12.61 GWh from wind and solar to the network annually. With the major objective of maximizing the renewable energy fraction in meeting the EV loads, a scheduling algorithm was developed for charging the EVs connected to the network. With the proposed scheduling system, charging of EVs are prioritized during the periods of higher renewable energy generation, depending upon the state of charge (SOC) of the EVs. This resulted in a high renewable energy fraction of 71.56% even without the support of batteries or any other supplementary generation options. The proposed algorithm for EV charge scheduling is designed to be generic and flexible in which number & locations of the EVs, the battery capacity, connection status, state of charge, discharging agreements etc. can be modified to adapt it for any real-world situations. The proposed method is further being extended for the resource management of fast charging stations in the distribution networks as seen in Konara et al. (2023a, 2023b). The analysis can also be extended considering dynamic price of energy as a constraint in the schedule optimization.

Table 3
Comparison of the renewable energy fraction achieved by the proposed method with similar studies.

Study	Renewable energy systems	Tied to the main grid	Energy storage/other generation options	Renewable energy fraction
Singh and Kumar (2023)	Solar PV, Wind turbine	Yes	Battery and Diesel Generator	97.44%–98.53%
Allouhi and Rehman (2023)	Solar PV, Wind turbine	Yes	Battery	Up to 71.66%
Bilal et al. (2023)	Solar PV, Wind turbine	yes	Battery	Up to 100%
Ullah et al. (2023)	Solar PV	yes	No	63%
Rehman et al. (2023)	Solar PV	Yes	No	38.5%–55.6%
Zhang et al. (2023)	Solar PV, Wind turbine	Yes	No	48.57%–73.66%
Ampah et al. (2022)	Solar PV, Wind Turbine and Biomass Generator	No – Microgrid based	Battery and Biogas Generator	100%
Boddapati et al. (2022)	Solar PV, Wind turbine	No – Microgrid based	Battery and Diesel Generator	50%–61%
Himabindu et al. (2021)	Solar PV, Wind turbine	Yes	Battery	51.4 to 64.5
Alghoul et al. (2018)	Solar PV	Yes	Battery	67%
Present study	Solar PV, Wind turbine	Yes	No	71.56%

CRediT authorship contribution statement

Manuel S. Mathew: Conceptualization, Methodology, Software, Validation, Writing – original draft. **Mohan Lal Kolhe:** Supervision, Writing – original draft, Writing – review & editing. **Surya Teja Kandukuri:** Supervision, Writing – review & editing. **Christian W. Omlin:** Supervision, Writing – review & editing.

Declaration of competing interest

The authors declare that they have no known competing financial interests or personal relationships that could have appeared to influence the work reported in this paper.

Data availability

The data that has been used is confidential.

References

Alghoul, M., Hammadi, F., Amin, N., Asim, N., 2018. The role of existing infrastructure of fuel stations in deploying solar charging systems, electric vehicles and solar energy: a preliminary analysis. Technol. Forecast. Soc. Change 137, 317–326. https://doi.org/10.1016/j.techfore.2018.06.040.

Ali Saadon, A.-O., Tengku Juhana Tengku, H., Nur Azzammudin, R., Agileswari, K.R., Marayati Binti, M., Mohammad, F., Mahammad, A.H., 2019. Review on scheduling, clustering, and forecasting strategies for controlling electric vehicle charging: challenges and recommendations. IEEE Access 7, 128353–128371. https://doi.org/10.1109/ACCESS.2019.2939595.

Allouhi, A., Rehman, S., 2023. Grid-connected hybrid renewable energy systems for supermarkets with electric vehicle charging platforms: optimization and sensitivity analyses. Energy Rep. 9, 3305–3318. https://doi.org/10.1016/j.egyr.2023.02.005.

Alsabbagh, A., Wu, B., Ma, C., 2021. Distributed electric vehicles charging management considering time anxiety and customer behaviors. IEEE Trans. Ind. Inf. 17 (4), 2422–2431. https://doi.org/10.1109/TII.2020.3003669.

Alsabbagh, A., Yin, H., Ma, C., 2020. Distributed electric vehicles charging management with social contribution concept. IEEE Trans. Ind. Inf. 16 (5), 3483–3492. https://doi.org/10.1109/TII.2019.2950460.

Ampah, J.D., Afrane, S., Agyekum, E.B., Adun, H., Yusuf, A.A., Bamisile, O., 2022. Electric vehicles development in Sub-Saharan Africa: performance assessment of standalone renewable energy systems for hydrogen refuelling and electricity charging stations (HRECS). J. Clean. Prod. 376, 134238 https://doi.org/10.1016/j.jclepro.2022.134238.

Apostolaki-Iosifidou, E., Codani, P., Kempton, W., 2017. Measurement of power loss during electric vehicle charging and discharging. Energy 127 (C), 730–742. https://doi.org/10.1016/j.energy.2017.03.015.

Aswantara, I.K.A., Kab Seok, K., Sung, D.K., 2013. A Centralized EV Charging Scheme Based on User Satisfaction Fairness and Cost. IEEE, pp. 1–4. https://doi.org/10.1109/ISGT-Asia.2013.6698730.

Bilal, M., Ahmad, F., Rizwan, M., 2023. Techno-economic assessment of grid and renewable powered electric vehicle charging stations in India using a modified metaheuristic technique. Energy Convers. Manag. 284, 116995 https://doi.org/10.1016/j.enconman.2023.116995.

Boddapati, V., Kumar, A.R., Daniel, S.A., Padmanaban, S., 2022. Design and prospective assessment of a hybrid energy-based electric vehicle charging station. Sustain. Energy Technol. Assessments 53, 102389. https://doi.org/10.1016/j.seta.2022.102389.

Bu, F., Yuan, Y., Wang, Z., Dehghanpour, K., Kimber, A., 2019. A Time-Series Distribution Test System Based on Real Utility Data. https://doi.org/10.1109/NAPS46351.2019.8999982.

Ester, M., Kriegel, H.-P., Sander, J., Xu, X., 1996. A Density-Based Algorithm for Discovering Clusters in Large Spatial Databases with Noise. kdd, pp. 226–231.

Fix, E., Hodges, J.L., 1989. Discriminatory analysis. Nonparametric discrimination: consistency properties. Int. Stat. Rev. 57 (3), 238–247. https://doi.org/10.2307/1403797.

Himabindu, N., Hampannavar, S., Deepa, B., Swapna, M., 2021. Analysis of microgrid integrated Photovoltaic (PV) Powered Electric Vehicle Charging Stations (EVCS) under different solar irradiation conditions in India: a way towards sustainable development and growth. Energy Rep. 7, 8534–8547. https://doi.org/10.1016/j.egyr.2021.10.103.

Impram, S., Varbak Nese, S., Oral, B., 2020. Challenges of renewable energy penetration on power system flexibility: a survey. Energy Strategy Rev. 31, 100539 https://doi.org/10.1016/j.esr.2020.100539.

International Energy Agency, 2022a. Global EV Outlook 2022. International Energy Agency.

International Energy Agency, 2022b. Outlook for electricity. In: International Energy Agency. World Energy Outlook 2022. International Energy Agency.

International Energy Agency, 2022c. Renewable electricity. In: Agency, I.E. (Ed.), Renewables 2022. International Energy Agency.

Iowa State University, 2021. IEM::download ASOS/AWOS/METAR data. https://mesonet.agron.iastate.edu/request/download.phtml.

Kapoor, A., Patel, V.S., Sharma, A., Mohapatra, A., 2022. Centralized and decentralized pricing strategies for optimal scheduling of electric vehicles. IEEE Trans. Smart Grid 13 (3), 2234–2244. https://doi.org/10.1109/TSG.2022.3141261.

Konara, K.M.S.Y., Kolhe, M.L., Ulltveit-Moe, N., Balapuwaduge, I.A.M., 2023a. Optimal utilization of charging resources of fast charging station with opportunistic electric vehicle users. Batteries. https://doi.org/10.3390/batteries9020140.

Konara, K.M.S.Y., Kolhe, M.L., Ulltveit-Moe, N., Balapuwaduge, I.A.M., 2023b. Reliability enhancement of fast charging station under electric vehicle supply equipment failures and repairs. Energies. https://doi.org/10.3390/en16062933.

Mathew, S., 2006. Wind Energy: Fundamentals, Resource Analysis and Economics. Springer, 9783540309055.

Ministry of Transport, 2021. Norway is electric. https://www.regjeringen.no/en/topics/transport-and-communications/veg/faktaartikler-vei-og-ts/norway-is-electric/id2677481/ (Accessed 20 February 2023).

Moeini-Aghtaie, M., Abbaspour, A., Fotuhi-Firuzabad, M., 2014. Online multicriteria framework for charging management of PHEVs. IEEE Trans. Veh. Technol. 63 (7), 3028–3037. https://doi.org/10.1109/TVT.2014.2320963.

Muqbel, A., Al-Awami, A.T., Parvania, M., 2022. Optimal planning of distributed battery energy storage systems in unbalanced distribution networks. IEEE Syst. J. 16 (1), 1194–1205. https://doi.org/10.1109/JSYST.2021.3099439.

Paudel, A., Hussain, S.A., Sadiq, R., Zareipour, H., Hewage, K., 2022. Decentralized cooperative approach for electric vehicle charging. J. Clean. Prod. 364, 132590 https://doi.org/10.1016/j.jclepro.2022.132590.

Rahbari-Asr, N., Chow, M.-Y., 2014. Cooperative distributed demand management for community charging of PHEV/PEVs based on KKT conditions and consensus networks. IEEE Trans. Ind. Inf. 10 (3), 1907–1916. https://doi.org/10.1109/TII.2014.2304412.

Ramachandran, V., 2011. Modeling of Utility Distribution Feeder in OpenDSS with Steady State Impact Analysis of Distributed Generation. West Virginia University, 1267693975.

Rehman, A.U., Ullah, Z., Shafiq, A., Hasanien, H.M., Luo, P., Badshah, F., 2023. Load management, energy economics, and environmental protection nexus considering PV-based EV charging stations. Energy, 128332. https://doi.org/10.1016/j.energy.2023.128332.

Rouholamini, M., Wang, C., Nehrir, H., Hu, X., Hu, Z., Aki, H., Zhao, B., Miao, Z., Strunz, K., 2022. A review of modeling, management, and applications of grid-connected Li-ion battery storage systems. IEEE Trans. Smart Grid 13 (6), 4505–4524. https://doi.org/10.1109/TSG.2022.3188598.

Sachs, J., Lafortune, G., Fuller, G., Woelm, F., Kroll, C., 2022. Sustainable Development Report 2022. Cambridge University Press, 9781009210089.

Sharma, A., 2021. Techno-Economic Performance Evaluation of Photovoltaic Based Micro-grid with Energy Management Strategies. Universitetet i Agder.

Singh, B., Kumar, A., 2023. Optimal energy management and feasibility analysis of hybrid renewable energy sources with BESS and impact of electric vehicle load with demand response program. Energy 278, 127867. https://doi.org/10.1016/j.energy.2023.127867.

Taljegard, M., Göransson, L., Odenberger, M., Johnsson, F., 2019. Impacts of electric vehicles on the electricity generation portfolio – a Scandinavian-German case study. Appl. Energy 235, 1637–1650. https://doi.org/10.1016/j.apenergy.2018.10.133.

Triviño-Cabrera, A., Aguado, J.A., Torre, S.d.l., 2019. Joint routing and scheduling for electric vehicles in smart grids with V2G. Energy 175, 113–122. https://doi.org/10.1016/j.energy.2019.02.184.

Ullah, Z., Wang, S., Wu, G., Hasanien, H.M., Rehman, A.U., Turky, R.A., Elkadeem, M.R., 2023. Optimal scheduling and techno-economic analysis of electric vehicles by implementing solar-based grid-tied charging station. Energy 267, 126560. https://doi.org/10.1016/j.energy.2022.126560.

Van Kriekinge, G., De Cauwer, C., Sapountzoglou, N., Coosemans, T., Messagie, M., 2021. Peak shaving and cost minimization using model predictive control for uni- and bi-directional charging of electric vehicles. Energy Rep. 7, 8760–8771. https://doi.org/10.1016/j.egyr.2021.11.207.

Veena, R., Mathew, S., Petra, M., 2020. Artificially intelligent models for the site-specific performance of wind turbines. Int. J. Energy Environ. Eng. 11, 289–297. https://doi.org/10.1007/s40095-020-00352-2.

Visakh, A., Selvan, M.P., 2021. Charging-Cost Minimization of Electric Vehicles and its Impact on the Distribution Network. IEEE, pp. 1–5. https://doi.org/10.1109/ICPS52420.2021.9670292.

Zhang, G., Dai, M., Zhao, S., Zhu, X., 2023. Orderly automatic real-time charging scheduling scenario strategy for electric vehicles considering renewable energy consumption. Energy Rep. 9, 72–84. https://doi.org/10.1016/j.egyr.2022.11.164.

Zhao, T., Ding, Z., 2017. Distributed initialization-free cost-optimal charging control of plug-in electric vehicles for demand management. IEEE Trans. Ind. Inf. 13 (6), 2791–2801. https://doi.org/10.1109/TII.2017.2685422.